A Study on the Forming of CICC for the Superconducting Tokamac Device With Post-Forming Predictions via Virtual Manufacturing

Yeong Sung Suh, Cheon Seog Yoon, Sun Woong Choi, Hyunki Park, and Keeman Kim

***Abstract*—To construct the magnet assembled with the CICC (Cable-In-Conduit Conductor) for the superconducting Tokamak fusion device, the 3-roll bending, that inherently has a difficulty to form the coil with accurate radius of curvature, is used for continuous winding. This difficulty is mainly caused by the spring back after forming. In order to obtain precise dimension, a trial-and-error operation is inevitable. To reduce the effort of tryout, a relation between travel of the bending roller and post-forming displacement was obtained via virtual manufacturing. The radius of CICC after forming was expressed as a function of the bend-roll travel. In addition, the variation of the CICC cross-section (reduction of the conduit cross-section) was investigated during the first turn and during conduit bending with largest curvature to check if the strand can have enough space. To ensure the validity of the computation, prototype coils were manufactured and the coil radii after forming were measured. The data showed similar pattern with some discrepancy for large-sized coils. The residual stress generated by jacketing on the coil before roll bending was measured to investigate if its existence influences the final deformation behavior. A mapping function was proposed to compensate the error caused by the numerical assumptions.**

***Index Terms*—3-roll bending, CICC, magnet, spring back, virtual manufacturing.**

I. Introduction

THE CICC is a central solenoid model coil used in the superconducting Tokamak fusion device. The KSTAR magnet system has CS, PF, and TF coil configurations as presented in Fig. 1. To construct the magnet, 3-roll bending machine displayed in Fig. 2 is used in order to wind the coil continuously. The 3-roll bending is very simple to manipulate to form a straight pipe into a hoop. However, because of the spring back after forming, it inherently has a difficulty to form the coil with accurate radius of curvature. In order to obtain precise dimension, a trial-and-error operation is inevitable. With the rapid progress of computer and software technology, virtual manufacturing can drastically reduce this difficulty. The virtual manufacturing involves the use of a computer to simulate not only a product but also its manufacturing processes. Usually, virtual manufacturing utilizes nonlinear finite-element analysis to provide optimization of factors such as manufacturability, final shape, residual stress, and life-cycle estimations, etc.

Fig. 1. Several coil configurations and winding schemes used in the KSTAR superconducting magnet: (a) CS coil (b) PF coil (c) TF coil.

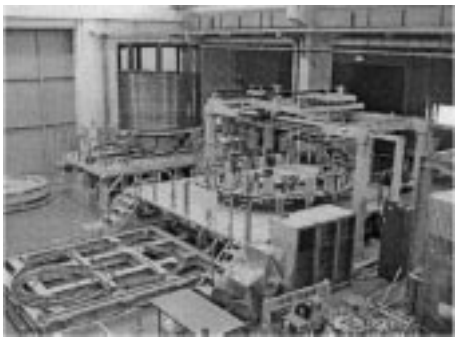

Fig. 2. KSTAR magnet winding machine using 3-roll bending process (Energy Lab, SAIT, Taejon).

In this work, the CICC was virtually manufactured by simulating the 3-roll bending process with ABAQUS so that the final geometry of CICC can be accurately obtained with a minimum effort. Fig. 3 is a schematic of the 3-roll bending process. As the drive rollers push the CICC, it proceeds in the forming direction. With the bend roller the CICC is formed into a circle with a constant radius of curvature. There are various sizes of CICC in the Tokamac device, the radius of which ranges from 431 mm (CS) to 3850 mm (PF). The downward travel of bending roller versus final radius of CICC after spring back was monitored. The radius of CICC after forming was expressed as a function of the bend-roll travel. Two different materials, Incoloy 908 and SUS 304 were employed in the calculation.

In addition, the variation of the CICC cross-sectional area was investigated during the first turn and during the conduit bending with the largest curvature to check if the superconducting strand can secure enough space. If the reduction is too high, the strand that will be packed inside the conduit may be damaged. It is regulated that the area of reduction should not be greater than 1.5% based on the results of stability and mechanical analysis [1], [2].

Manuscript received September 24, 2001. This work was supported in part by the Korean Ministry of Science and Technology.

Y. S. Suh, C. S. Yoon, and S. W. Choi are with the Department of Mechanical Engineering, Hannam University, Taejon, Korea (e-mail: suhy@mail.hannam.ac.kr).

H. Park and K. Kim are with the Energy Lab., Samsung Advanced Institute of Technology, Taejon, Korea (e-mail: hkpark@venus.sait.samsung.co.kr).

Publisher Item Identifier S 1051-8223(02)04280-X.

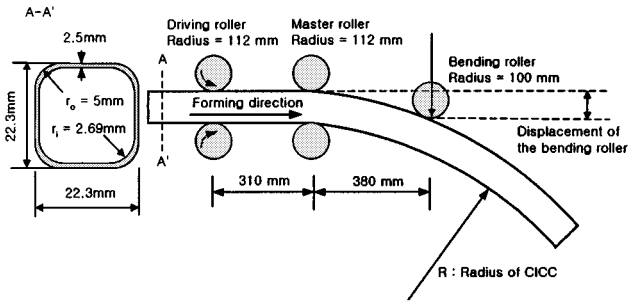

Fig. 3. Schematics of 3-roll bending process to form CICC.

TABLE I
MECHANICAL PROPERTIES OF SUS 304 (MEASURED) AND INCOLOY 908 [3]

Symbol	SUS 304	Incoloy 908
Elastic Modulus	195 GPa	180 GPa
Poisson's Ratio	0.3	0.3
Yield Stress	321 MPa	848 MPa
Effective Stress-Strain	$\sigma = 1525.5(0.03978 + \varepsilon^p)^{0.483}$	$\sigma = 1848.3(0.00334 + \varepsilon^p)^{0.137}$

Also, in order to predict the likelihood of SAGBO (Stress Accelerated Grain Boundary Oxidation) on the conduit, the maximum von Mises stress was monitored. The SAGBO occurs when the operating temperature ranges from 550 °C to 800 °C, tensile strength is greater than 200 MPa, and the oxygen pressure is greater than 10^{-5} torr (at 1 atm, 0.14 ppm) simultaneously [1].

To examine the accuracy of the computation, prototype coils without strands were manufactured and the coil radii after forming were measured. The residual stress in the coil, which had been generated during jacketing and straightening processes before roll bending, was measured to investigate if its magnitude is large enough to influence the final deformation behavior.

II. APPROACH

A. Virtual Manufacturing

CS coils were modeled. As a virtual manufacturing engine, ABAQUS, a commercial nonlinear FEM package was used on Compaq-Digital workstation 433AU and SGI Origin 2000. To reduce cpu time, only the longitudinal half of the entire configuration was modeled. The shell element was preferred to the brick element since the former is less stiff, accommodating shear deformation through thickness due to bending. Therefore, S4R element was used to model the CICC in 3 dimensions. Five integration points were assigned in the thickness direction to take account of an appropriate shear deformation during bending. For rollers, rigid definition was used using *RIGID SURFACE option which defines rigid surface analytically. The friction was assumed only between driving rollers and the CICC.

After spring back, the coordinate of three-points of the CICC was monitored. These numbers were put into the Intelli-CAD (a commercial 2D CAD program) and the radius of the virtually manufactured CICC was automatically calculated. The relation between the travels of the bending roller versus radius of CICC was obtained by fitting the calculated data. The cross-sectional area and the von Mises stress at the deformed CICC with minimum radius of curvature were monitored. The mechanical properties of two materials used are included in Table I.

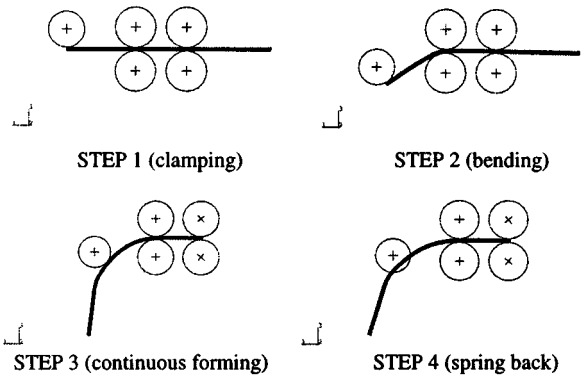

Fig. 4. Stepwise-deformed shape of CICC with downward bending roller travel of 200 mm (Material: Incoloy 908).

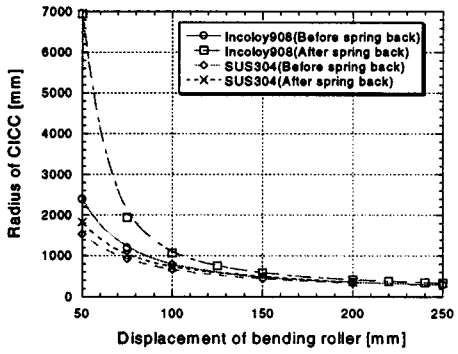

Fig. 5. Predicted radius of formed CICC after spring back versus displacement of the bending roller for both Incoloy 908 and SUS304. Monitoring points were taken near the master rollers.

B. Manufacturing of Prototype CICC

In order to check the accuracy of the computation, several prototype CICC was manufactured. The CNC roll-bending machine installed in SAIT, as shown in Fig. 2, was used. Only the stainless steel CICC without superconducting strands was formed. The post-forming radius was measured with specially designed apparatus.

C. Measurement of Residual Stresses

The hole-drilling strain gage method of stress relaxation was used for the measurement of residual stresses [4], [5]. The strain gage used was Tokyo Sokki Kenkyujo FRS-3-11. The empty CICC was cut by an appropriate size such that the length was determined as more than ten times of hole-diameter to minimize edge and end effects. The strain gage was attached on four different locations: welding, wall, opposite-to-welding, and fillet surfaces.

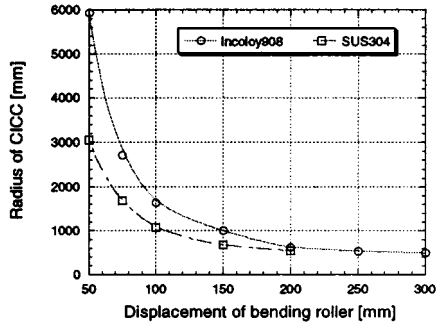

Fig. 6. Predicted radius of formed CICC after spring back versus distance of the bending roller for both Incoloy 908 and SUS304. Monitoring points were taken near the bending rollers.

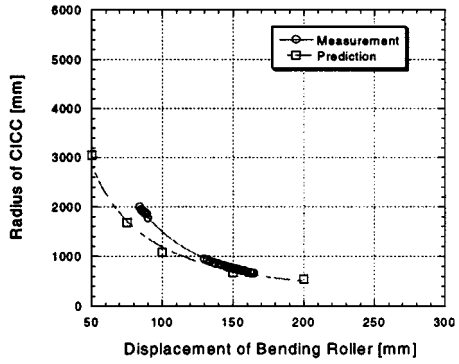

Fig. 7. Measured and predicted data. Material used was SUS 304.

III. Results and Discussions

A. Vertical Displacement of the Bending Roller versus Final Radius of CICC After Spring Back

Stepwise-deformed shape of CICC with downward bending roller travel of 200 mm is presented in Fig. 4. The driving rollers were set to rotate with 4.02 rad in order for the CICC precedes 450 mm. Fig. 5 shows the predicted radius of formed CICC after spring back versus distance of the bending roller for both Incoloy 908 and SUS304. The coil with Incoloy 908 shows more spring back and it is more magnificent as the radius of the coil increases. In the numerical experiment of similar case [6], it was reported that the coil radius due to spring back would be increased when yield stress, coil radius, and tube thickness are increased, and when elastic modulus and cross-sectional tube diameter are decreased. This is consistent with the current results as the yield stress of Incoloy 908 is greater than that of the SUS 304. Fig. 5 was obtained by taking three points near master rollers. Since the distribution of residual stress on the coil was observed to be somewhat nonuniform (This indicates that the forming is not steady state yet and needs longer feeding), the monitoring points were moved toward the bending rollers. This showed a little change of the curve patterns as presented in Fig. 6.

During the simulation, it was found that it would be very difficult to form small sized coils such as CS (431 mm) with the present layout configuration. Therefore, the bending roller was suggested to move toward the master rollers. By doing so, the smaller radius of curvature can be obtained with ease. The maximum von Mises on the unloaded and curved CICC was approximately 500∼600 MPa and the maximum tensile stress 500 MPa, which surpasses the SAGBO criteria. Since the operating temperature is in the ranges vulnerable to SAGBO, it was concluded that controlling the oxygen pressure is the only way to avoid it.

TABLE II
Measured Principal Stresses and Their Direction

	σ_{MAX} [MPA]	σ_{MIN} [MPA]	α_{MIN} [°]
Surface 1	203.7	78.6	2.3
Surface 2	296.2	36.5	-9.1
Surface 3	175.7	111.1	-40.3
Surface 4	305.7	65.3	0.5

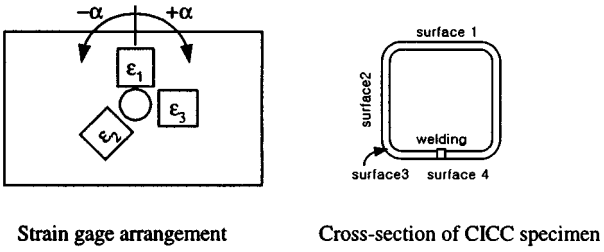

Fig. 8. Schematic of strain gage arrangements and locations.

B. Thickness Variation of the CICC

Thickness variation was negligible during forming. For example, when the travel distance of the bending roller was 250 mm (Material: Incoloy 908), the thickness varied from 2.40 mm to 2.59 mm (original thickness was 2.5 mm).

C. Cross-Sectional Area of CICC With Minimum Radius

The CICC with the minimum radius was observed to be the location where the pipe is bent with nearly right angle, see Fig. 1(a). The minimum radius was assumed to be 250 mm. To check the area reduced from the worst condition, the radius of master roller was increased to 200 mm to accommodate 250 mm-radius of CICC after spring back. The monitored nodes were selected near the lower master roller. The travel of the bending roller was 250 mm. With Incoloy 908, the radii before and after the spring back were 198 mm and 234 mm. Therefore, the section on the arc radius 198 mm (i.e., before spring back) was examined in order to calculate the sectional area. The area was defined as the one surrounded by the perimeter of centerline through the thickness direction. The area was reduced to 375.6 mm^2 that is 0.63% reduction with respect to the original area, 378 mm^2. Therefore, it was predicted that the area reduction during forming might be neglected. Similar results were obtained with SUS 304.

D. Prototype Manufacturing and Comparison of Spring Back Data

Fig. 7 shows the data from both virtual and real manufacturing. Only the case with SUS 304 was compared. Both data showed close proximity except for the larger radii.

It was conjectured that this error would have caused by the embedded residual stresses generated during jacketing and straightening processes. In other words, if the magnitude of

the embedded residual stress is not negligible, the subsequent plastic deformation cannot erase it completely. For smaller size coils, the plastic deformation is relatively greater than the larger ones. Therefore, embedded residual stress may not have greater influence on the subsequent deformation in this case.

In order to check if the magnitude of the residual stress is influential, the residual stress was measured. Table II includes measured principal stresses and their directions. The schematic of strain gage arrangements and locations are presented in Fig. 8. The results show that the magnitude of residual stress is greater than the minimum bound of SAGBO criteria in most measured locations. Overall, the results indicate that the residual stresses generated during the fabrication of the CICC cannot be overlooked.

Since the residual stress cannot be taken account correctly into the virtual manufacturing, this has to be compensated in some way. Roughly, this can be corrected mathematically based on the pattern shown in Fig. 7. That is, the expression for the measured data is:

$$f(Y) = 3.0000 \times 10^{6} Y^{-1.6607} \tag{1}$$

where Y is the displacement of the bending roller. And the one from the computation is

$$g(Y) = 3.9299 \times 10^{5} Y^{-1.2594}. \tag{2}$$

In order to map $g(Y)$ to $f(Y)$, a mapping function $h(Y)$ can be assumed as following form:

$$f(Y) = g(Y)h(Y). \tag{3}$$

Solving this, following expression for $h(Y)$ was obtained:

$$h(Y) = 7.6338 Y^{-0.4013}. \tag{4}$$

Using this mapping function, the virtual manufacturing data can match with the real data. This function compensates overlooked assumptions that can hardly be conjectured without the experiment.

IV. Conclusions

A relation between travel of the bending roller and spring back radius was obtained via virtual manufacturing with 3-roll bending process. For use as an initial input for the real manufacturing, the radius of CICC after forming was expressed as a function of the bend-roll travel. The calculation was performed for Incoloy and SUS304. The maximum von Mises stress after spring back was also monitored to predict the likelihood of SAGBO. Finally, the variation of the CICC cross-section (reduction of the conduit cross-section) was investigated for the worst cases. With the largest curvature, the cross-sectional area was not much reduced. The spring back data were compared with the ones from prototype manufacturing. The results showed good proximity except with the larger radii. The measurement of residual stress on CICC before roll bending revealed that its influence on the computation was not negligible. Therefore, experimental calibration by introducing the mapping function was proposed. Using it, the virtual manufacturing data can be more effectively used for accurate manufacturing by compensating overlooked assumptions made in the numerical computation.

References

[1] S. H. Kim, "Development of the central solenoid (CS) model coil with Nb_3Sn cable-in-conduit (CIC) superconductor for the superconducting Tokamak fusion device," Ph.D. dissertation (in Korean), Seoul National University, 1999.

[2] S.-H. Kim, K.-H. Chung, and D. K. Lee, "A continuous winding scheme for superconducting Tokamac coils with cable-in-conduit conductor," *Fusion Engineering and Design*, vol. 55, no. 21, 2001.

[3] L. S. Toma, M. M. Steeves, and R. P. Reed, "Incoloy alloy 908 data handbook," in *PFC/RR-94-2*. Superconducting Magnet Development Group, Plasma Fusion Center: MIT, 1994.

[4] ASTM, "Determining residual stresses by the hole-drilling strain-gage method," *Annual Book of ASTM*, vol. E837-89, p. 730, 1981.

[5] M. Beghini and L. Bertini, "Recent advances in the hole drilling method for residual stress measurement," *Journal of Materials Engineering and Performance*, vol. 7, p. 163, 1998.

[6] Y. W. Kim and J. I. Kim, "An analysis to minimize the amount of spring back after coiling of helical steam generator tubes," *Int. J. Pressure Vessels and Piping*, vol. 78, p. 11, 2001.